




Lubricated Wear Properties of Zn-30Al-3Cu-Si Alloys

TEMEL SAVAŞKAN¹ and HASAN ONUR TAN ^{2,3}

1.—Department of Mechanical Engineering, Haliç University, 34060 Eyüpsultan, Istanbul, Turkey. 2.—Department of Mechanical Engineering, Giresun University, 28200 Giresun, Turkey. 3.—e-mail: hasan.tan@giresun.edu.tr

To assess the effect of silicon content (SC) and test parameters on the lubricated wear of Zn-30 wt.% Al-3 wt.% Cu-(0.5–5) wt.% Si alloys, six quaternary alloys were produced by casting. Their wear properties were investigated at different ranges of contact pressure (CP) of 1–8 MPa and sliding velocity (SV) of 1–3 ms⁻¹ for two different sliding distances (SD) of 20 km and 108 km. It was observed that Si addition (SA) improved the tribological properties of Zn-30Al-3Cu alloy, but an increase in the SC above a certain percentage (0.5%) adversely affected these properties. Therefore, Zn-30Al-3Cu-0.5Si alloy demonstrated the lowest friction coefficient (FC) and wear volume (WV) among the alloys tested. The correlations between the lubricated wear properties (FC and WV) of the alloys and test conditions (CP and SV) were made by non-linear regression analysis using the wear test data. Finally, the equations for the relationship between the wear properties of the alloys and the test parameters were determined.

INTRODUCTION

Extensive studies on monotectoid Zn-Al-based alloys during the 1940s led to the development of a commercial alloy named ALZEN 305 (Zn-30Al-5Cu).^{1–7} This alloy was also called white bronze and demonstrated a relatively low FC, high wear resistance (WR), low specific weight, good embeddability, high damping capacity, and stable pricing.^{1,5,6} These alloys have found wide range of usage in several engineering applications.^{8–14} However, their copper content (CC) is considerably high, and copper is a relatively expensive strategic metal.^{15–17} Therefore, later studies concentrated on the determination of the optimum CC of this alloy. Following recent systematic research about the influence of copper addition on the structure and properties of binary Zn-30Al alloy, a new ternary alloy (Zn-30Al-3Cu) was developed.^{18,19} This alloy exhibited a higher quality index value and WR than ALZEN 305 alloy and SAE 660 bronze.¹⁹ This means that a small amount (2%) of reduction in the CC of ALZEN 305 not only provides economic advantages but also improves its tribological properties. Later work

revealed that the addition of silicon increases the hardness of this alloy, but reduces its strength and ductility.²⁰ However, silicon additions had no regular influence on the dry wear properties of this alloy.²⁰ These observations were referred to the distribution, size, and volume fraction of the hard and brittle silicon particles.²⁰ This implies that the SC of Zn-30Al-3Cu-Si alloys should be optimized for engineering and tribological applications. However, no research has been conducted on the lubricated wear characteristics of Si-containing Zn-30Al-3Cu-based alloys. Therefore, the aim of this work is to study the lubricated wear characteristics of Zn-30Al-3Cu-Si alloys at different contact pressures (CPs) and sliding velocities (SVs) and determine the optimum SC and operating parameters for plain bearing applications.

MATERIALS AND METHODS

Zn-30 wt.% Al-3 wt.% Cu-(0.5–5) wt.% Si alloys were produced by metal mold casting using pure aluminum, zinc, and master alloys of Al-50 wt.% Cu and Al-12 wt.% Si. Their chemical compositions were determined by optical emission spectroscopy method. The microstructures of these alloys were studied using a scanning electron microscope (SEM), and their phases were determined by energy

(Received November 6, 2023; accepted March 26, 2024)

dispersive spectroscopy (EDS) and X-ray diffraction techniques as reported in the published articles and thesis.^{18–20}

The hardness (H), strength, and ductility of the alloys were measured by hardness, tensile, compression, and impact tests as described in detail in the previously published articles and thesis.^{18–20} The H of the alloys was measured using a Rockwell tester, and the readings were subsequently converted to Brinell hardness number (BHN). Tensile and compression tests were performed on the cylindrical specimens at a strain rate of $4 \times 10^{-3} \text{ s}^{-1}$ according to TS 138 EN 10002-1 (ASTM E-8) and TS EN 206 (ASTM E-9) standards, respectively. At least three tests were performed to calculate the mean values of H, ultimate tensile strength (UTS), percent elongation (PE), and compressive strength (CS) of the alloys. Lubricated wear properties of the alloys were studied using a block-on-disk type tester whose technical drawing is given in Fig. 1. The wear tests were conducted at an oil flow rate (OFR) of $1 \text{ cm}^3 \text{ h}^{-1}$ and in the ranges of CP of 1–8 MPa and SV of $1\text{--}3 \text{ ms}^{-1}$ for a SD of 20 km. To study the influence of SD on the wear properties of the alloys, long-distance (108 km) tests were carried out at an OFR of $1 \text{ cm}^3 \text{ h}^{-1}$, CP of 6 MPa, and SV of 2 ms^{-1} . Some wear tests were repeated twice to check the reliability of the experimental data. However, the differences between the measurements were observed to be not greater than 2% of the average value of the properties. This indicates that the measurement error or the extent of variation had no significant influence on the shape and order of the wear curves plotted.

RESULTS

The chemical compositions of the alloys determined by arc spark optical emission spectroscopy are given in Table I. SEM micrographs of Zn-30Al-3Cu-0.5Si, Zn-30Al-3Cu-3Si, and Zn-30Al-3Cu-5Si

alloys are given in Fig. 2a–c, respectively. These micrographs show that the microstructure of these alloys is composed of β dendrites together with eutectoid reaction products of $\alpha + \eta$ phases and ε (CuZn_4) and Si particles. The effects of SC on the mechanical properties of the alloys are shown in Fig. 3.

The FC and WV versus SD curves for Zn-30Al-3Cu-(0.5–5)Si alloys subjected to wear tests at an OFR of $1 \text{ cm}^3 \text{ h}^{-1}$, CP of 6 MPa, and SV of 2 ms^{-1} for a total SD of 108 km are shown in Fig. 4. These curves show that the FC of the alloys becomes almost constant after an SD of about 20 km, following an instant increment and a sharp decrement at the start of the test run (Fig. 4a). However, their WV reached a steady state after an SD of approximately 60 km following an initial increase (Fig. 4b).

The curves of FC and WV versus SC for the alloys tested at an OFR of $1 \text{ cm}^3 \text{ h}^{-1}$, CP of 6 MPa, and SV of 2 ms^{-1} for an SD of 20 km are shown in Fig. 5. The FC and WV of the alloys show quite a sharp increment with increasing SC, but when the SC exceeds 2%, the rate of increase decreases and both properties reach almost steady states.

Table I. Chemical composition of the alloys

Alloy	Chemical composition (wt.%)			
	Zn	Al	Cu	Si
Zn-30Al-3Cu	67.1	29.8	3.1	–
Zn-30Al-3Cu-0.5Si	66.4	30.2	2.9	0.5
Zn-30Al-3Cu-1Si	66.7	29.9	2.9	1.1
Zn-30Al-3Cu-2Si	66.1	30.1	3.1	1.9
Zn-30Al-3Cu-3Si	63.9	30.2	3	2.9
Zn-30Al-3Cu-4Si	63.1	30.1	2.9	3.9
Zn-30Al-3Cu-5Si	61.7	30.1	3.1	5.1

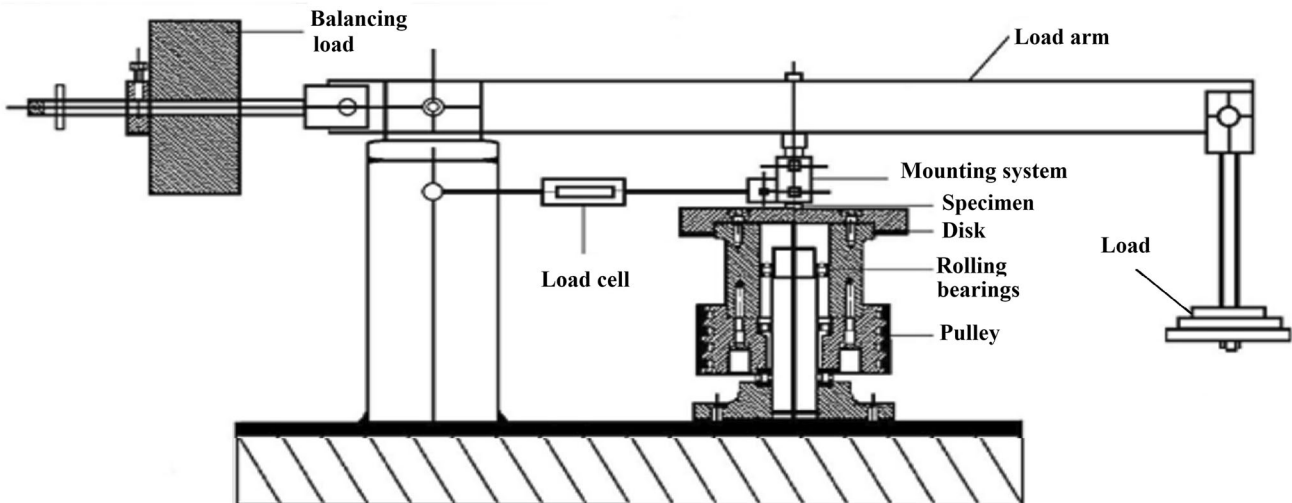


Fig. 1. Technical drawing of the wear tester.

Lubricated Wear Properties of Zn-30Al-3Cu-Si Alloys

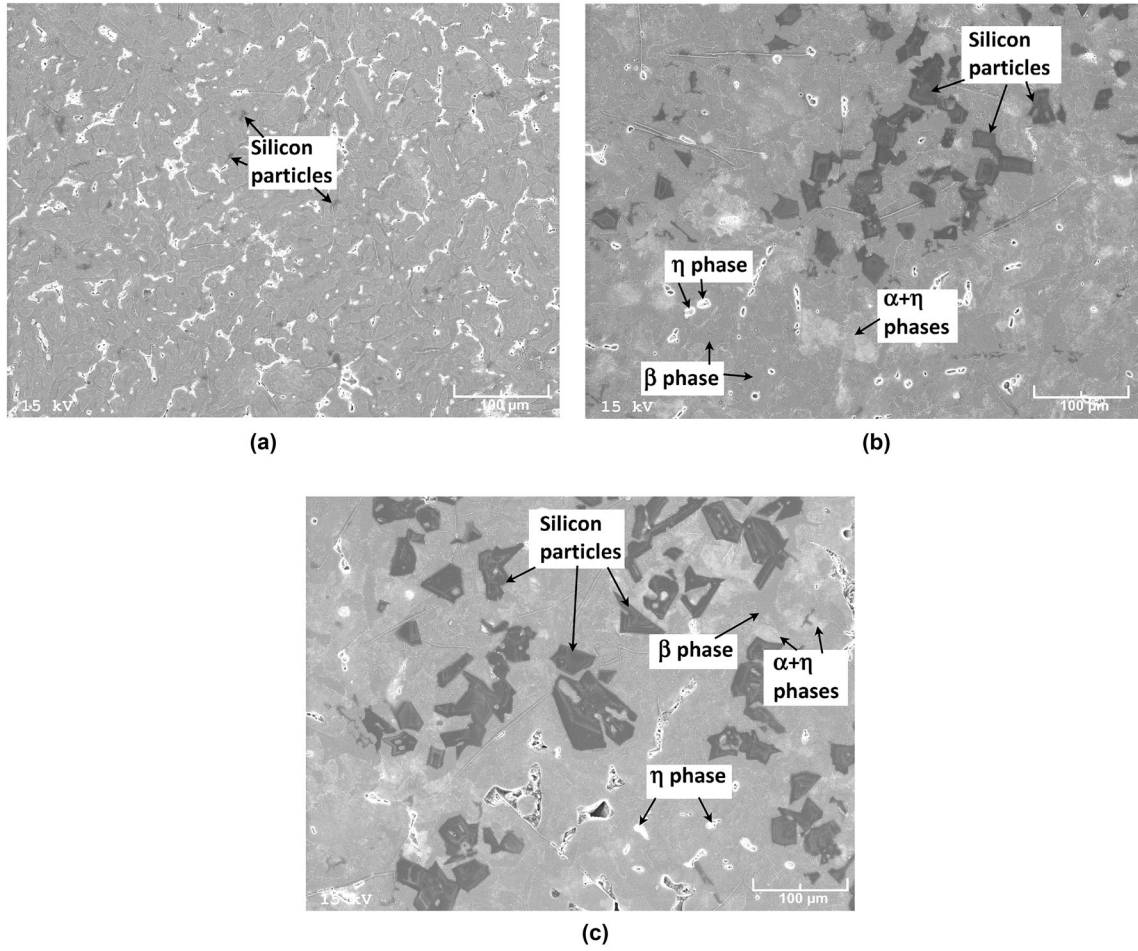


Fig. 2. SEM micrographs of (a) Zn-30Al-3Cu-0.5Si, (b) Zn-30Al-3Cu-3Si, and (c) Zn-30Al-3Cu-5Si alloys.

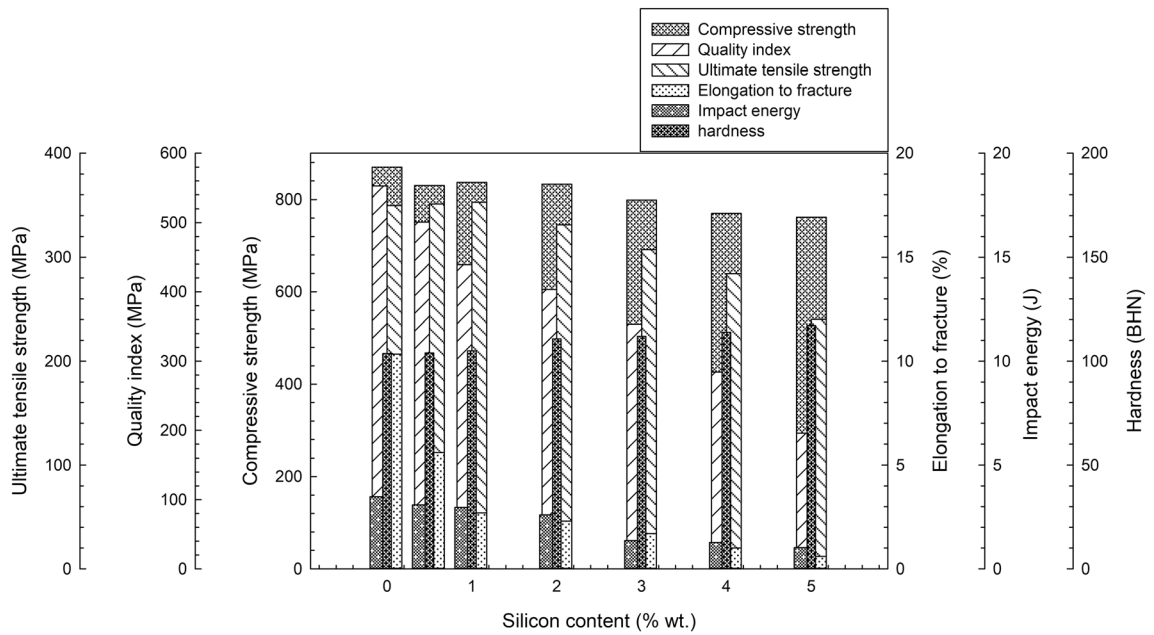


Fig. 3. Bar charts show the effect of silicon content on the mechanical properties of Zn-30Al-3Cu-Si alloys.

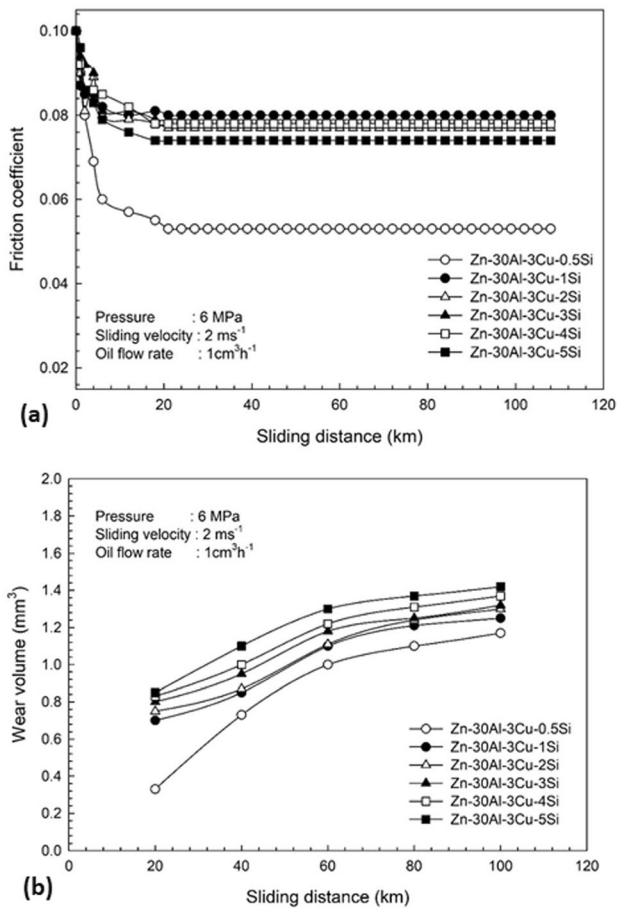


Fig. 4. Curves represent the variations in (a) FC and (b) WV of Zn-30Al-Cu-(0.5-5)Si alloys with SD.

The curves of FC and WV versus CP for the alloys are presented in Fig. 6. These curves show that the FCs of the alloys decrease, but their WVs increase with increasing CP.

The curves of FC and WV versus SV for the alloys are shown in Fig. 7. These curves demonstrate that the FC and WV of the alloys increase almost linearly with increasing SV, but the values of these properties of Zn-30Al-3Cu-0.5Si alloy show the lowest rate of increase.

The three-dimensional (3D) graphs illustrating the changes in FC and WV with both SC and SD are given in Fig. 8. The FC and WV of the alloys exhibited a non-linear increase with increasing SC after showing their lowest levels at 0.5% Si.

The 3D graphs showing the changes in FC and WV with both SC and CP are given in Fig. 9. The FC of the alloys increases with increasing SC but decreases as the CP increases (Fig. 9a). However, the rates of increase in their WV with SC and CP were observed to be quite different from each other (Fig. 9b).

Three-dimensional plots illustrating the changes in FC and WV with both SC and SV are given in Fig. 10. These plots show that the FC and WV values of the alloys increase with increasing SC, starting from their lowest levels at 0.5% Si. These properties of the alloys increase almost linearly with SV.

SEM views of the wear surface of Zn-30Al-3Cu-0.5Si and Zn-30Al-3Cu-5Si alloys tested at an OFR of 1 cm³ h⁻¹, CP of 6 MPa, and SV of 2 ms⁻¹ for a SD of 108 km are shown in Fig. 11. Scratches and smeared regions were observed on their worn

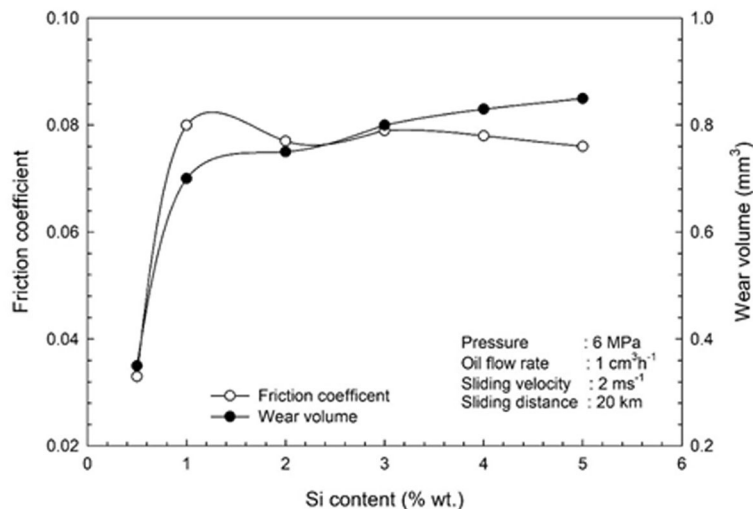


Fig. 5. Curves show the variations in FC and WV of the alloys with SC.

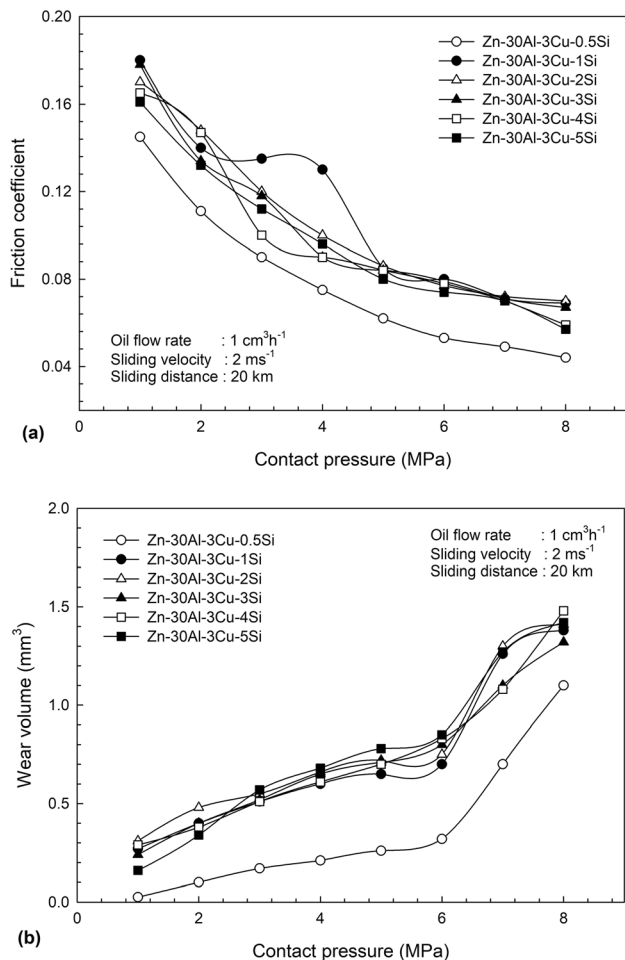


Fig. 6. Curves show the changes in (a) FC and (b) WV with CP for the alloys.

surfaces, and as the SC increased the area of the smeared regions increased and the scratches became more pronounced.

DISCUSSION

The FC of the alloys subjected to wear tests at an OFR of 1 cm³ h⁻¹, CP of 6 MPa, and SV of 2 ms⁻¹ for an SD of 108 km decreased rapidly and reached a steady state after approximately 20 km following a sudden initial increase, as shown in Fig. 4a. However, their WVs reached steady states following a sharp rise at the early stage of the tests (Fig. 4b). The rapid decrease in FC of the alloys at the start of the wear tests can be attributed to the transition from dry to lubricated sliding, and the increment in their WV results from asperity contact owing to insufficient thickness of the oil film during the wear-in period.^{21–24} However, when the oil film thickness becomes adequate to separate the surfaces of the sample and the disk during the test, both the FC and the WV of the alloys reach steady states.^{23,24}

The FC and the WV of the alloys showed a sharp rise with increasing SC, but they reached steady states above 2% Si (Fig. 5). This finding may result

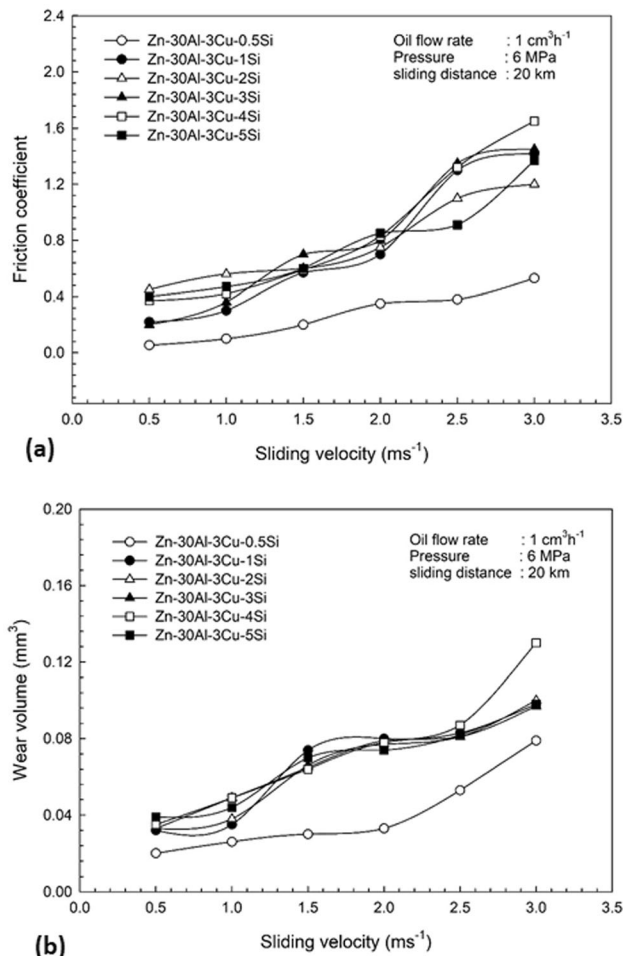


Fig. 7. Curves show the variations in (a) FC and (b) WV with SV for the alloys tested.

from the brittleness and hardening effect of Si particles. Brittleness causes an increase in FC and the WV, but this increment can be balanced with a hardness increase.^{21,25–27} This is probably why these properties reach steady states above 2% Si.

The FC of the alloys tested at a constant OFR of 1 cm³ h⁻¹ and an SV of 2 ms⁻¹ decreased, but their WV increased with increasing CP, as shown in Fig. 6. This finding can be related to the effect of hydrodynamic lubrication during the wear tests. It is known that under hydrodynamic lubrication the FC decreases with increasing CP.^{23,24,28} As the CP increases, the thickness of the oil film between the contacting surfaces decreases. This, in turn, causes a decrease in the friction between the oil molecules, giving rise to a decrease in the FC. However, the increase in the WV with increasing CP can be attributed to the asperity contact and the increase in friction force and heat which occurs especially during the running-in period.^{23,24,28}

The FC and WV of the alloys tested at a constant OFR of 1 cm³ h⁻¹ and CP of 6 MPa increased with increasing SV, but this increase became more prominent above a certain level of SV (2 ms⁻¹), as

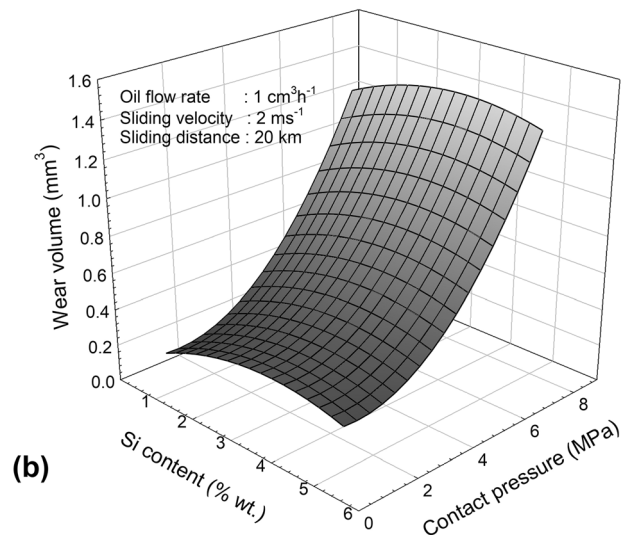
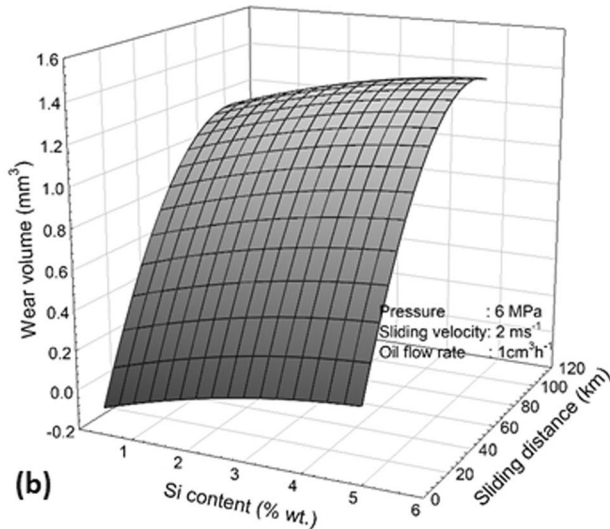
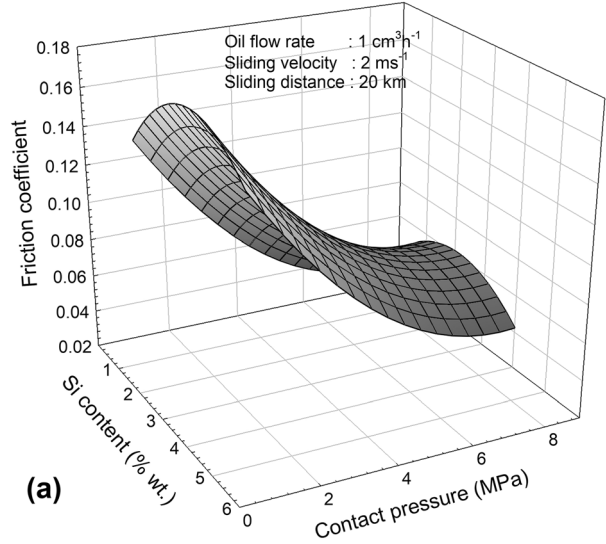
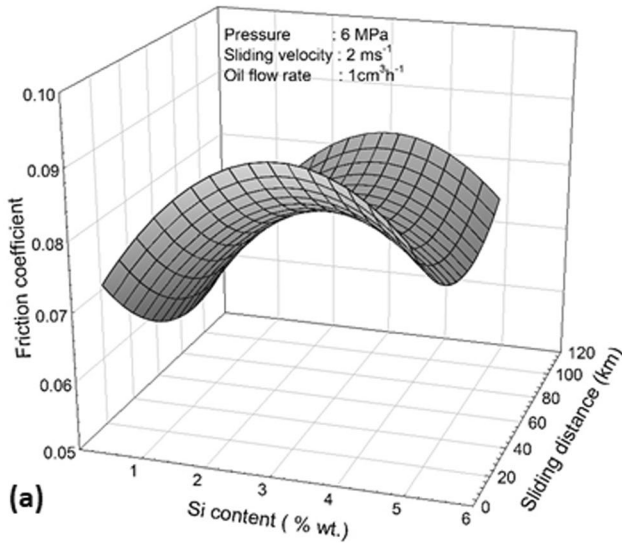


Fig. 8. Three-dimensional plots show the changes of (a) FC and (b) WV values with SC and SD for Zn-30Al-3Cu-(0.5-5)Si alloys subjected to lubricated wear tests.

Fig. 9. Three-dimensional plots showing the change of (a) FC and (b) WV values with SC and CP for the alloys subjected to lubricated wear tests.

shown in Fig. 7. This finding can be related to the centrifugal force acting on the oil and the change in the viscosity of the oil. As the sliding velocity rises, the centrifugal force acting on the lubricating oil increases. The increase in the centrifugal force leads to an increment in the amount of oil removed from the disk surface and the friction between the oil molecules. This can give rise to an increment in the FC by decreasing the amount of oil or the oil film thickness between the disk and the specimen surfaces. The frictional heat generated during operation cannot be adequately dissipated by the oil. Furthermore, as the SV increases it becomes difficult to dissipate the frictional heat because of insufficient time. This means that as the SV increases, the temperature of the alloy samples increases. An increment in operating temperature

causes a decrement in the viscosity of the oil. This can also cause an increase in the FC by facilitating the removal of oil from the disk surface. The increment in the WV may be related to the asperity contact that occurs during the running-in period. As the SV increases, the centrifugal force acting on the lubricating oil increases. An increase in the centrifugal force causes a delay in the formation of a sufficient oil film thickness by giving rise to an increment in the amount of oil removed from the disk surface. This delay causes an increase in the WV of the alloys by increasing the duration of asperity contact between the sample and disk surfaces.

The relationships showing the effects of SC together with (a) SD, (b) CP, and (c) SV on the lubricated FC and WV of Zn-30Al-3Cu-Si alloys

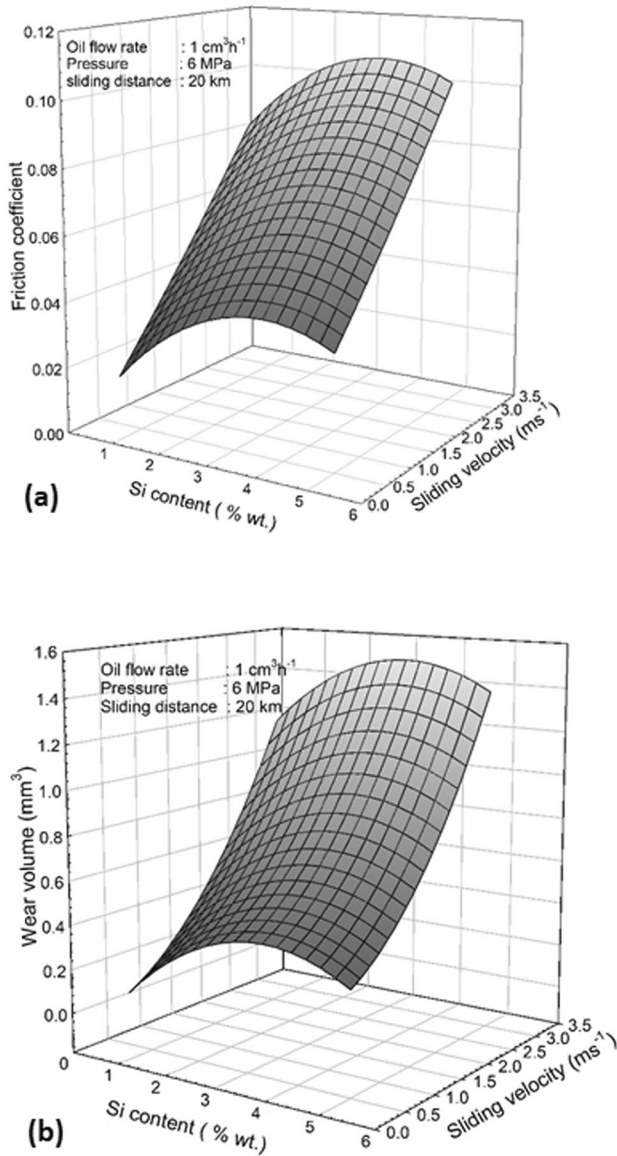


Fig. 10. Three-dimensional graphs show the changes in (a) FC and (b) WV values with SC and SV for the alloys subjected to lubricated wear tests.

determined by non-linear regression analysis of the wear test data used to plot the 3D graphs are given below:

(a)

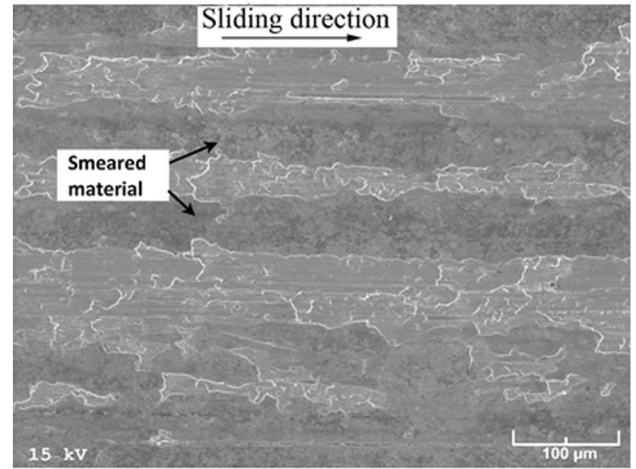
$$\begin{aligned} \mu &= 0.067 + 0.017Si - 0.0004d - 0.003Si^2 & (r^2 = 0.76) \\ \Delta V &= -0.111 + 0.101Si + 0.028d - 0.0086Si^2 - 0.0002d^2 & (r^2 = 0.96) \end{aligned}$$

(b)

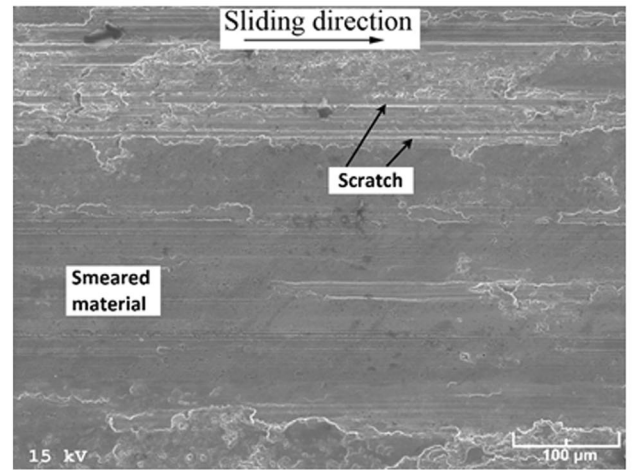
$$\begin{aligned} \mu &= 0.149 + 0.034Si - 0.033p - 0.005Si^2 + 0.002p^2 & (r^2 = 0.82) \\ \Delta V &= 0.106 + 0.073Si - 0.041p - 0.005Si^2 + 0.022p^2 & (r^2 = 0.81) \end{aligned}$$

(c)

$$\begin{aligned} \mu &= -0.006 + 0.019Si + 0.023v - 0.002Si^2 & (r^2 = 0.86) \\ \Delta V &= -0.129 + 0.284Si + 0.062v - 0.042Si^2 + 0.108v^2 & (r^2 = 0.90) \end{aligned}$$



(a)



(b)

Fig. 11. Worn surfaces of (a) Zn-30Al-3Cu-0.5Si and (b) Zn-30Al-3Cu-5Si alloys tested at an OFR of 1 cm³ h⁻¹, CP of 6 MPa, and SV of 2 ms⁻¹ for a SD of 108 km.

where μ is friction coefficient, ΔV is wear volume (mm³), Si is silicon content (wt.%), d is sliding distance (m), v is sliding velocity (ms⁻¹), and p is contact pressure (MPa). The coefficient of determination (r^2) values for the above equations were found to be between 0.76 and 0.9. This means that the reliability of the proposed equations changes from 76% to 90%. The parameters (μ , ΔV , Si, d , v , and p) of these equations have the same meanings as the acronyms used in the main text as FC, WV, SC, SD, SV, and CP, respectively.

SEM images revealed the scratches and smeared and adhered material on the worn surface of the experimental alloys (Fig. 11). It was also observed that as their SC increased, the area of the smeared regions and the quantity of the scratches increased (Fig. 11). This finding can be attributed to the presence of hard and brittle silicon particles in the alloys. Additionally, it is known that both the number and the size of the silicon particles increase as the SC

increases.^{21,29–31} The removal of these hard particles from the wear surface can result in an increase in the quantity and width of the scratches due to their abrasive nature. Smearred material and scratches can be taken as evidence of adhesive and abrasive wear, respectively.^{20,31} Therefore, it may be stated that adhesion and abrasion dominate the lubricated wear of the alloys tested.

CONCLUSIONS

The conclusions drawn from the current study on lubricated wear of Zn-30Al-3Cu-Si alloys are given below:

1. The friction coefficient and wear volume of the experimental alloys show a sharp initial increment with increasing silicon content, but both properties reach steady states above a Si content of 2%.
2. The friction coefficient of the alloys tested decreases, but their wear volume increases with increasing contact pressure while their friction coefficient and wear volume increase with increasing sliding velocity.
3. Zn-30Al-3Cu-0.5Si alloy exhibits the lowest friction coefficient and wear volume among the alloys tested. This finding indicates that Si addition improves the tribological properties of Zn-30Al-3Cu alloy, but the silicon content should not exceed 0.5%.
4. The relationships between the friction coefficient or wear volume of Zn-30Al-3Cu-Si alloys and test conditions can be expressed by the quadratic equations given in the Discussion section.
5. Adhesion and abrasion are the effective mechanisms for the wear of the experimental alloys.

FUNDING

Open access funding provided by the Scientific and Technological Research Council of Türkiye (TÜBİTAK).

CONFLICT OF INTEREST

The authors declare that they have no conflict of interest.

OPEN ACCESS

This article is licensed under a Creative Commons Attribution 4.0 International License, which permits use, sharing, adaptation, distribution and reproduction in any medium or format, as long as you give appropriate credit to the original author(s) and the source, provide a link to the Creative Commons licence, and indicate if changes were made. The images or other third party material in this article are included in the article's Creative Commons licence, unless indicated otherwise in a credit line to the material. If material is not included in the article's Creative Commons licence

and your intended use is not permitted by statutory regulation or exceeds the permitted use, you will need to obtain permission directly from the copyright holder. To view a copy of this licence, visit <http://creativecommons.org/licenses/by/4.0/>.

REFERENCES

1. W. Mihaichuk, *Mach. Des.* 53, 133 (1981).
2. K.M.W. Köster, *Z. Metallkd.* 33, 248 (1941).
3. E. Gebhardt, *Z. Metallkd.* 32, 78 (1940).
4. E. Gervais, R.J. Barnhurst, and C.A. Loong, *JOM* 37, 43 <https://doi.org/10.1007/BF03258743> (1985).
5. A.F. Skenazi, J. Pelerin, D. Coutsouradis, B. Magnus, and M. Meeus, *Metall* 37, 898 (1983).
6. S. Murphy, and T. Savaskan, *Wear* 98, 151 [https://doi.org/10.1016/0043-1648\(84\)90224-2](https://doi.org/10.1016/0043-1648(84)90224-2) (1984).
7. Voestalpine, Alzen 305, Alzen 501, *White Bronze* (1976).
8. S.S. Liu, H. Tu, C.J. Wu, J.H. Wang, and X.P. Su, *Mater Today Commun.* <https://doi.org/10.1016/j.mtcomm.2021.102564> (2021).
9. Z.C. Wu, S. Sandlobes, L. Wu, W.P. Hu, G. Gottstein, and S. Korte-Kerzel, *Mater Sci Eng A-Struct* 651, 675 <https://doi.org/10.1016/j.msea.2015.11.020> (2016).
10. M.D. de Medeiros, R. Septimio, C.A.P. da Silva, J.E. Spinelli, N. Cheung, A. Garcia, and B.L. Silva, *Mater Char.* <https://doi.org/10.1016/j.matchar.2021.110936> (2021).
11. W.K. Krajewski, A.L. Greer, J. Buraś, G. Piwowarski and P.K. Krajewski, In *Materials Today: Proceedings*, (2019), pp. 306–311.
12. I. Peter, M. Agapie, and B. Varga, *Metals.* <https://doi.org/10.3390/met8110924> (2018).
13. M. Babic, B. Stojanovic, D. Dzunic, and M. Pantic, *J. Compos. Mater.* 54, 2113 <https://doi.org/10.1177/0021998319891766> (2020).
14. A. Pola, M. Tocci, and F.E. Goodwin, *Metals.* <https://doi.org/10.3390/met10020253> (2020).
15. LME, “London Metal Exchange”, <https://www.lme.com/en/>.
16. T. Economics, “Trading Economics”, <https://tradingeconomics.com>.
17. HKEX, “Hong Kong exchanges and clearing market”, http://www.hkex.com.hk/?sc_lang=en.
18. H.O. Tan, and T. Savaşkan, *J. Mater. Eng. Perform.* 29, 4794 <https://doi.org/10.1007/s11665-020-04976-7> (2020).
19. T. Savaşkan, and H.O. Tan, *Arch. Metall. Mater.* 68, 607 <https://doi.org/10.24425/amm.2023.142441> (2023).
20. H.O. Tan, In *Mechanical Engineering Graduate Program*, (Karadeniz Technical University: 2019), p 158.
21. Z. Azakli, and T. Savaskan, *Tribol. Int.* 41, 9 <https://doi.org/10.1016/j.triboint.2007.04.002> (2008).
22. O. Bican, and T. Savaşkan, *Tribol. Lett.* 37, 175 <https://doi.org/10.1007/s11249-009-9509-4> (2010).
23. I. Hutchings and P. Shipway, *Tribology: friction and wear of engineering materials*, (Butterworth-Heinemann, 2017).
24. J. Halling, *Principles of tribology*, (Macmillan International Higher Education, 1978).
25. Y. Alemdağ, and T. Savaşkan, *Tribol. Lett.* 29, 221 <https://doi.org/10.1007/s11249-008-9299-0> (2008).
26. B.K. Prasad, *Mater Char.* 44, 301 [https://doi.org/10.1016/S1044-5803\(99\)00057-1](https://doi.org/10.1016/S1044-5803(99)00057-1) (2000).
27. B.K. Prasad, *Mater. Trans. JIM* 38, 701 <https://doi.org/10.2320/matertrans1989.38.701> (1997).
28. B. Bhushan, *Principles and Applications of Tribology* (1999).
29. T. Savaskan, and O. Bican, *Mater. Sci. Eng. A* 404, 259 <https://doi.org/10.1016/j.msea.2005.05.078> (2005).
30. T. Savaskan, and Z. Azakli, *Wear* 264, 920 <https://doi.org/10.1016/j.wear.2007.06.008> (2008).
31. T. Savaskan, A.P. Hekimoglu, Z. Azakli, and M. Calis, *J. Tribol.* <https://doi.org/10.1115/1.4051264> (2022).

Publisher's Note Springer Nature remains neutral with regard to jurisdictional claims in published maps and institutional affiliations.